



Control of slow-light effect in a metamaterial-loaded Si waveguide

MAKOTO TANAKA,¹ TOMOHIRO AMEMIYA,^{1,2,*} HIBIKI KAGAMI,¹
NOBUHIKO NISHIYAMA,^{1,2} AND SHIGEHISA ARAI^{1,2}

¹*Department of Electrical and Electronic Engineering, Tokyo Institute of Technology, 2-12-1 O-okayama, Meguro-ku, Tokyo 152-8552, Japan*

²*Institute of Innovative Research, Tokyo Institute of Technology, 2-12-1 O-okayama, Meguro-ku, Tokyo 152-8552, Japan*

**amemiya.t.ab@m.titech.ac.jp*

Abstract: A metamaterial is an artificial material designed to control the electric permittivity and magnetic permeability freely beyond naturally existing values. A promising application is a slow-light device realized using a combination of optical waveguides and metamaterials. This paper proposes a method to dynamically control the slow-light effect in a metamaterial-loaded Si waveguide. In this method, the slow-light effect (i.e., group index) is controlled by changing the phase of the control light incident on the device from a direction opposite to that of the signal light. The group index of the device could be continuously controlled from 63.6 to 4.2 at a wavelength of 1.55 μm .

© 2020 Optical Society of America under the terms of the [OSA Open Access Publishing Agreement](#)

1. Introduction

Metamaterials comprising periodically arranged metal nanostructures can exhibit extraordinary optical properties not existing in nature [1,2]. This unique property enables to develop innovative technologies for sophisticated optical manipulation such as sub-diffraction-limit lenses, the storage of broadband light, and invisibility cloaking [3–8]. Introducing the concept of metamaterials to waveguide optics has opened a novel field—magnetic permeability design—for semiconductor photonic integrated circuits [9–13]. Tassin et al. [14] and Tsakmakidis et al. [15] conducted pioneering studies in this field; they discovered a phenomenon called the slow-light effect in permeability-controlled waveguides induced by the negative Goos–Hänchen shift. Subsequently, various attempts have been made to create novel photonic devices using a combination of waveguides and metamaterials, including the “trapped rainbow” light storage device [16], unidirectional mode converters [17], waveguide-integrated mode selective antennas [18], and ultra-compact optical modulator [19].

Inspired by the above results, we proposed a method to delay optical signals using a silicon-wire waveguide with a metamaterial on its surface [20]. This method takes advantage of the slow-light effect in the waveguide induced by a steep wavelength dispersion in the metamaterial. The optical signal can be significantly delayed simply by attaching a metamaterial (split ring resonator) onto the surface of the waveguide [21].

To use the above device as a functional device, it is indispensable to dynamically control the slow-light effect with an external signal. However, once the shape of a metamaterial is decided, it is difficult to change its optical properties. To this end, two promising approaches have been proposed: one is changing the shape of the metamaterial using micro-electro-mechanical systems (MEMS) [22] and the other is changing the characteristics of the material surrounding the metamaterial [23–27]. In both the cases, the device structure becomes complicated, and the compatibility with the conventional silicon optical circuit is poor.

In this paper, we propose a completely different approach to control the slow-light effect.

2. Proposal of optically controlled method of the slow-light effect in metamaterial-loaded Si waveguides

Figure 1 shows the schematics of the proposed method. In this method, the control light is incident on a metamaterial-loaded Si waveguide (i.e., slow-light waveguide) [20,21] from a direction opposite to that of the signal light, and a standing wave is generated in the waveguide. Here, the node position of the standing wave is controlled by changing the phase of the control light, and the magnitude of the interaction between the light and the metamaterial can be continuously controlled. For example, when the control light is incident such that the signal light and the control light are in phase at the center of the metamaterial, the signal light is strongly affected by the wavelength dispersion in the metamaterial and exhibits a slow-light effect (Fig. 1(a)). On the other hand, when the control light is incident such that the signal light and the control light are out of phase at the center of the metamaterial, the propagation characteristics of the signal light strongly reflect those of a normal Si waveguide (Fig. 1(b)). Compared with the conventional dynamic control methods for metamaterials, the proposed method does not require an advanced control function to be added to the metamaterial itself, and the operation speed is higher.

Figure 2 shows an example of optical buffering realized using this method. In this system, we consider using a Si-based ring reflector with the metamaterial-loaded waveguide, an optical phase shifter, and a Y-splitter. After input light signal is equally divided by the Y-splitter, one is directly input to the metamaterial-loaded waveguide, and the other is input to the same region through the phase shifter from the opposite direction (a length of the metamaterial-loaded waveguide is smaller than one bit length of the input signal (10-40 Gbit/s)). Here, the output signal is completely the same as the input signal because one loop in the reflector is exactly the same in both clockwise and counterclockwise directions. Separately from that, a time delay occurs in the output signal depending on the state of standing wave in the metamaterial-loaded waveguide. When the state of standing wave in the metamaterial-loaded waveguide is set as shown in Fig. 1(a) by controlling the phase shifter, the slow-light effect is obtained and the output signal is delayed by several bits. On the contrary, when the state of standing wave in the metamaterial-loaded waveguide is set as shown in Fig. 1(b), optical buffering is released. An

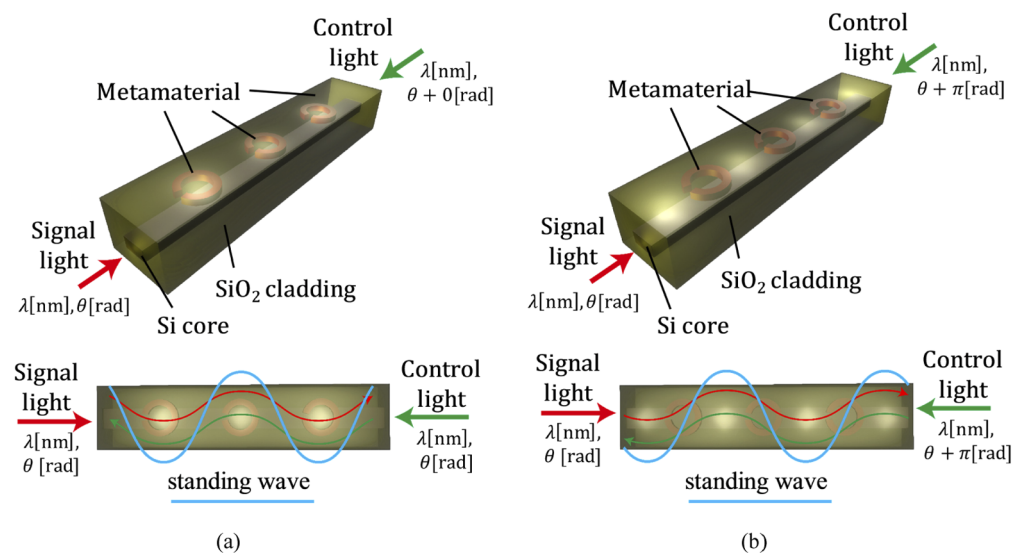


Fig. 1. (a)(b) Optical control of the group index of a metamaterial-loaded Si waveguide by tuning the initial phase offset of two counter-propagating incident lights.

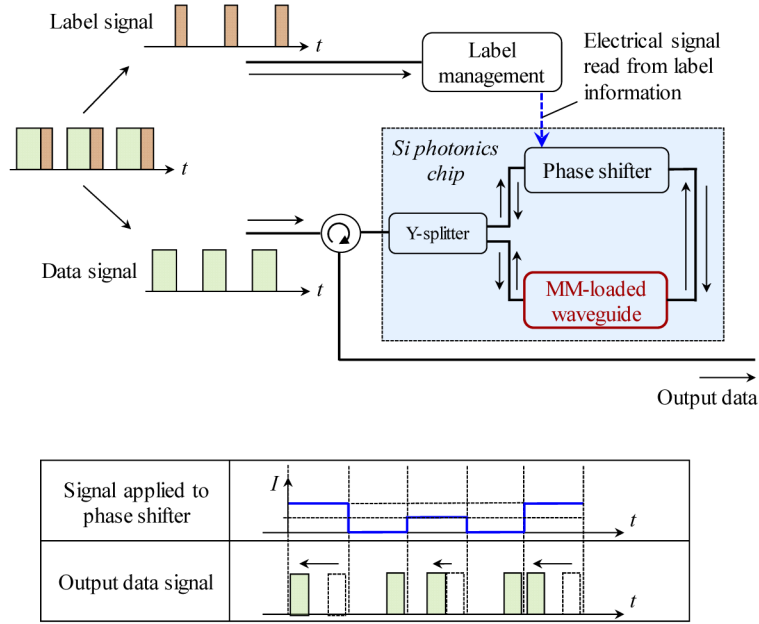


Fig. 2. Example of optical buffering using a metamaterial-loaded Si waveguide.

electrical input corresponding to the header information is given to the phase shifter so that an appropriate delay time for each signal can be obtained.

3. Analysis method for slow-light control of metamaterial waveguides

3.1. Metamaterial waveguide theory

In this study, the dispersion relationship of the metamaterial-loaded Si waveguide was established by conducting a homogenization mode analysis [28] to reduce the significant calculation time. In the homogenization mode analysis, we replaced the metamaterial and its neighborhood with a hypothetical uniform layer with appropriate permittivity and permeability values (see Fig. 3(a)). In a waveguide including the layer with anisotropic permittivity and permeability, the wave equation for a TE-mode light can be written as

$$\frac{\partial^2 E_x}{\partial y^2} + \left(\omega^2 \varepsilon_0 \mu_0 \varepsilon_x \mu_z - \beta^2 \frac{\mu_z}{\mu_y} \right) E_x = 0, \quad (1)$$

$$H_z = \frac{1}{j\omega \mu_0 \mu_z} \frac{\partial E_x}{\partial y}. \quad (2)$$

where β is the propagation constant of the device along the z -direction, ω is the angular frequency, ε_0 is the permittivity of vacuum, μ_0 is the permeability of vacuum, and E_x and H_z are the electric field parallel to the x axis and magnetic field parallel to the z axis of the light, respectively. We find from Eqs. (1) and (2) that E_x , H_z , and β are given by

$$\begin{pmatrix} E_x \\ H_z \end{pmatrix} \Big|_{top} = \prod_m \begin{pmatrix} \cosh(\beta_m d_m) & j\omega \mu_0 \mu_{zm} / \beta_m \cdot \sinh(\beta_m d_m) \\ \beta_m / j\omega \mu_0 \mu_{zm} \cdot \sinh(\beta_m d_m) & \cosh(\beta_m d_m) \end{pmatrix} \cdot \begin{pmatrix} E_x \\ H_z \end{pmatrix} \Big|_{bottom}, \quad (3)$$

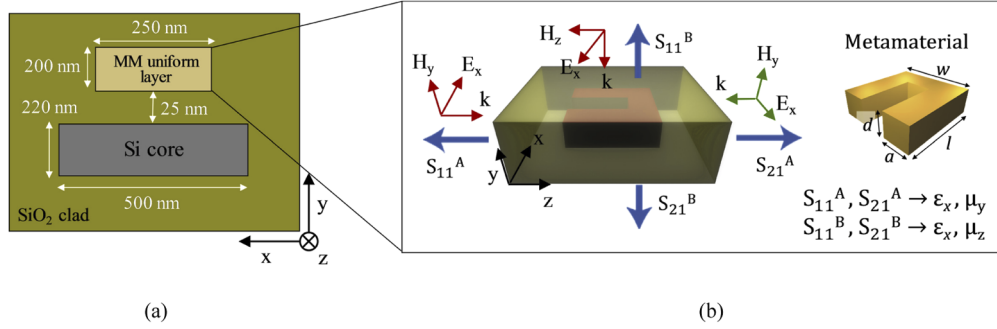


Fig. 3. (a) Cross section of a waveguide with a metamaterial uniform layer with appropriate values of permittivity and permeability; (b) retrieval of permittivity and permeability values from S parameters.

$$\beta_m = \sqrt{\beta^2 \frac{\mu_{zm}}{\mu_{ym}} - \omega^2 \epsilon_0 \mu_0 \epsilon_{xm} \mu_{zm}}, \quad (4)$$

where ϵ_{xm} is the x element of the relative permittivity tensor, μ_{ym} and μ_{zm} are the y and z elements of permeability tensors in the m -th layer, respectively, and d_m is the thickness of the m -th layer. At optical frequencies, the permeability tensors can be expressed using the identity matrix except in the metamaterial uniform layer. Assuming an exponential decrease in E_x and H_z , outside a waveguide, we can solve Eq. (3) and obtain the effective refractive index ($= \beta/\omega\sqrt{\epsilon_0\mu_0}$). Combining this method with the conventional equivalent-index method enables mode field analysis of the metamaterial-loaded waveguides shown in Fig. 3(a).

The effective values of ϵ_x , μ_y , and μ_z of the metamaterial uniform layer can be determined from the scattering parameters around the metamaterial calculated for incident plane waves introduced along the y and z directions. As shown in Fig. 3(b), ϵ_x and μ_y can be determined from S_{11}^A and S_{21}^A , ϵ_x and μ_z can be determined from S_{11}^B and S_{21}^B .

3.2. General formula for extracting the optical constitutive parameters of metamaterials with two counter-propagating incident light waves

Although there is a highly versatile formula for extracting the optical constitutive parameters of metamaterials from S-parameters, this formula cannot be used when two lights are inputted from opposite directions, i.e., it works only when light is inputted from one direction [29]. Therefore, in this section, we derive the general formula for extracting the optical constitutive parameters of metamaterials with two counter-propagating incident light waves

In Fig. 4, the electric field parallel to x axis of input 1 is given by

$$E_{1x}(\mathbf{r}, t) = (Ae^{ik_+ \cdot \mathbf{r}} + Be^{ik_- \cdot \mathbf{r}})e^{-i\omega t}, \quad (5)$$

where $\mathbf{k}_+ = (k_x, 0, k_z)$, $\mathbf{k}_- = (k_x, 0, -k_z)$ are wave vectors, A and B are the amplitudes of the forward and backward propagating light, respectively. Using the effective complex refractive index n , Eq. (5) is rearranged as follows:

$$E_{1x}(z, t) = (Ae^{inkz} + Be^{-inkz})e^{-i\omega t}. \quad (6)$$

where k is wavenumber in z direction, ω is angular frequency. Substituting Eq. (6) into Maxwell's equation

$$\nabla \times \mathbf{E} = i\omega\mu_0\mu\mathbf{H}(z, t). \quad (7)$$

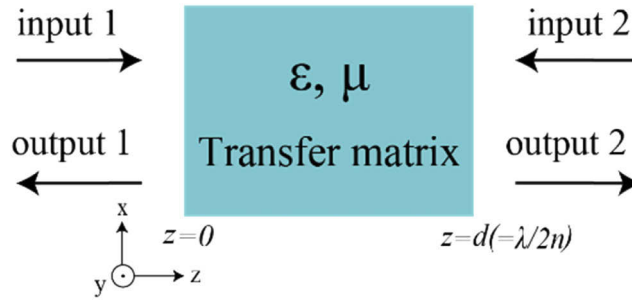


Fig. 4. Two ports model for retrieving constitutive parameters of the metamaterial uniform layer.

gives the following equation:

$$H_{\text{red1}}(z, t) = -\frac{ink}{\mu}(Ae^{inkz} - Be^{-inkz})e^{-i\omega t}. \quad (8)$$

where $H_{\text{red1}}(z, t) = i\omega\mu_0 H_y(z, t)$ is the magnetic field parallel to y axis of input 1, μ is the effective permeability. Substituting $z=0$ into Eqs. (6) and (8) gives the following equation:

$$E_1(0, t) = (A + B)e^{-i\omega t}, \quad (9)$$

$$H_{\text{red1}}(0, t) = -\frac{ink}{\mu}(A - B)e^{-i\omega t}. \quad (10)$$

From Eqs. (9) and (10), we have

$$Ae^{-i\omega t} = \frac{1}{2} \left\{ E_1(0, t) - \frac{\mu}{ink} H_{\text{red1}}(0, t) \right\}, \quad (11)$$

$$Be^{-i\omega t} = \frac{1}{2} \left\{ E_1(0, t) + \frac{\mu}{ink} H_{\text{red1}}(0, t) \right\} e^{-i\omega t}. \quad (12)$$

On the other hand, assuming that the electric and magnetic fields of the input 2 have the phase difference ϕ with respect to input 1, we have

$$E_2(z, t) = e^{i\phi} \{ B e^{ink(z-d)} + A e^{-ink(z-d)} \} e^{-i\omega t}, \quad (13)$$

$$H_{\text{red2}}(z, t) = -\frac{ink}{\mu} e^{i\phi} \{ B e^{ink(z-d)} - A e^{-ink(z-d)} \} e^{-i\omega t}. \quad (14)$$

In this study, length z of the metamaterial uniform layer was set to $c/2nf$ (c : speed of light, n : refractive index, f : incident frequency) because the position of the node of the standing wave needs to match the array pitch of metamaterials in the device. Therefore, using Eqs. (9), (10), (13), and (14), the electric and magnetic fields at an arbitrary position z are

$$E(z, t) = E_1(z, t) + E_2(z, t) = \{ A - B e^{i\phi} \} e^{inkz} + \{ B - A e^{i\phi} \} e^{-inkz} e^{-i\omega t}, \quad (15)$$

$$H_{\text{red}}(z, t) = H_{\text{red1}}(z, t) + H_{\text{red2}}(z, t) = \left[-\frac{ink}{\mu} \{ A - B e^{i\phi} \} e^{inkz} + \frac{ink}{\mu} \{ B - A e^{i\phi} \} e^{-inkz} \right] e^{-i\omega t}. \quad (16)$$

Substituting Eqs. (11) and (12) into Eqs. (13) and (14), we have

$$E(z, t) = (1 - e^{i\phi})\cos(nkz)E_1(0, t) - (1 + e^{i\phi})\frac{\mu}{nk}\sin(nkz)H_{\text{red}1}(0, t), \quad (17)$$

$$H_{\text{red}}(z, t) = (1 - e^{i\phi})\frac{nk}{\mu}\sin(nkz)E_1(0, t) + (1 + e^{i\phi})\cos(nkz)H_{\text{red}1}(0, t). \quad (18)$$

From Eqs. (17) and (18), we have the following **T**-matrix:

$$\begin{bmatrix} E(z, t) \\ H_{\text{red}}(z, t) \end{bmatrix} = \begin{bmatrix} T_{11} & T_{12} \\ T_{21} & T_{22} \end{bmatrix} \begin{bmatrix} E_1(0, t) \\ H_{\text{red}1}(0, t) \end{bmatrix} = \begin{bmatrix} (1 - e^{i\phi})\cos(nkz) & -(1 + e^{i\phi})\frac{\mu}{nk}\sin(nkz) \\ (1 - e^{i\phi})\frac{nk}{\mu}\sin(nkz) & (1 + e^{i\phi})\cos(nkz) \end{bmatrix} \begin{bmatrix} E_1(0, t) \\ H_{\text{red}1}(0, t) \end{bmatrix}. \quad (19)$$

From the **T**-matrix, each element of the **S**-matrix can be obtained as follows:

$$S_{11} = \frac{-2e^{i\phi}\cos(nkz) - i\left\{\frac{\mu}{n}(1 + e^{i\phi}) - \frac{n}{\mu}(1 - e^{i\phi})\right\}\sin(nkz)}{2\cos(nkz) - i\left\{\frac{\mu}{n}(1 + e^{i\phi}) + \frac{n}{\mu}(1 - e^{i\phi})\right\}\sin(nkz)}, \quad (20)$$

$$S_{12} = \frac{2(1 - e^{i2\phi})}{2\cos(nkz) - i\left\{\frac{\mu}{n}(1 + e^{i\phi}) + \frac{n}{\mu}(1 - e^{i\phi})\right\}\sin(nkz)}, \quad (21)$$

$$S_{21} = \frac{2}{2\cos(nkz) - i\left\{\frac{\mu}{n}(1 + e^{i\phi}) + \frac{n}{\mu}(1 - e^{i\phi})\right\}\sin(nkz)}, \quad (22)$$

$$S_{22} = \frac{2e^{i\phi}\cos(nkz) - i\left\{\frac{\mu}{n}(1 + e^{i\phi}) - \frac{n}{\mu}(1 - e^{i\phi})\right\}\sin(nkz)}{2\cos(nkz) - i\left\{\frac{\mu}{n}(1 + e^{i\phi}) + \frac{n}{\mu}(1 - e^{i\phi})\right\}\sin(nkz)}, \quad (23)$$

From Eqs. (20)–(23), the effective complex refractive index n and the effective complex impedance μ/n can be expressed as

$$n = \frac{1}{kd}\cos^{-1}\left\{\frac{1 - S_{11}^2 + S_{21}^2(1 + e^{i\phi})(1 - e^{i\phi})}{2S_{21}}\right\} = \sqrt{\varepsilon}\sqrt{\mu}, \quad (24)$$

$$\frac{\mu}{n} = \sqrt{\frac{(1 + S_{11})^2 - (1 - e^{i\phi})^2 S_{21}^2}{(1 - S_{11})^2 - (1 + e^{i\phi})^2 S_{21}^2}} = \frac{\sqrt{\mu}}{\sqrt{\varepsilon}}. \quad (25)$$

where k is the wave number of the incident light, d is the dimension of a unit cell of the metamaterial uniform layer, and ϕ is the phase difference between the two input lights. When the coefficients of $e^{i\phi}$ terms in Eqs. (24) and (25) are assumed 0 (i.e. in case with one incident light wave), they have the same form as the conventional formula [29].

In this study, ε_x and μ_y of the metamaterial uniform layer were derived from Eqs. (24) and (25) using the set of S_{11} and S_{21} shown in red in Fig. 3(b). μ_z was calculated by assuming that all coefficients of $e^{i\phi}$ terms in Eqs. (24) and (25) are 0.

4. Optically controlled slow-light effect in metamaterial-loaded Si waveguides

In this section, the actual device characteristics are analyzed based on the theory described in the previous section. Sections 4.1 and 4.2 discuss slow-light effects with and without control light. In Section 4.3, we show that the magnitude of the slow-light effect (the real part of the group index of the device) can be controlled continuously by changing the initial phase offset between the signal light and the control light, and also discuss an intrinsic loss of the device.

4.1. Constitutive parameters of metamaterial uniform layers without and with counter-propagating light

Figure 5 shows the values of the effective permittivity ϵ_x and permeability μ_y of the metamaterial uniform layer, calculated in the frequency range of 160–240 THz along the polarization direction of the incident light corresponding to those shown in Fig. 3(b). In the simulation, the dimensions of the individual ring were set as $l = 106$ nm, $w = 160$ nm, $a = 30$ nm, and $d = 30$ nm to ensure that the resonance occurs at an optical communication frequency of 193 THz (wavelength: 1.55 μm). The unit cell of the metamaterial uniform layer was assumed to be a cuboid with width $x = 200$ nm and height $y = 250$ nm (approximately one quarter of the wavelength or less). In addition, the length z of the uniform layer was set to $c/2nf$ (c : speed of light, n : refractive index, f : incident frequency), because the node position of the standing wave needs to match the array pitch of the metamaterials in the device.

In Fig. 5, the blue and red lines indicate the effective constitutive parameters without and with the counter-propagating light with a π phase offset, respectively. When there is no counter-propagating light (i.e., normal light propagation in the metamaterial-loaded Si waveguide), the permittivity and permeability exhibit a strong and sharp resonance at 193 THz, and all the parameters exhibit significant wavelength dispersion. The real part of μ_y varies from 0.105 to 22.238 on both sides of the resonance frequency line, and the metamaterial array shifts the permeability of its adjacent SiO_2 cladding away from 1.

In contrast, when the counter-propagating light with a π phase offset is incident from the opposite direction, the permittivity and permeability values (1.5 and 1, respectively) are almost constant. These values strongly reflect those of a pure SiO_2 bulk, because the nodes of the synthetic wave are located at the center of the metamaterials.

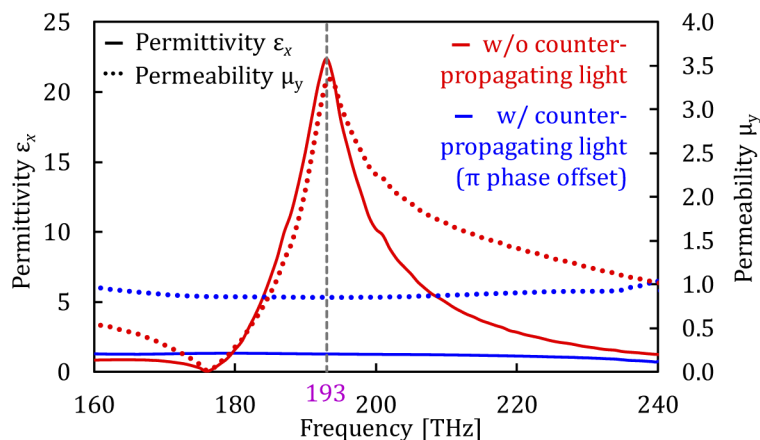


Fig. 5. Effective constitutive parameters of the metamaterial uniform layer without and with counter-propagating light with π phase offset.

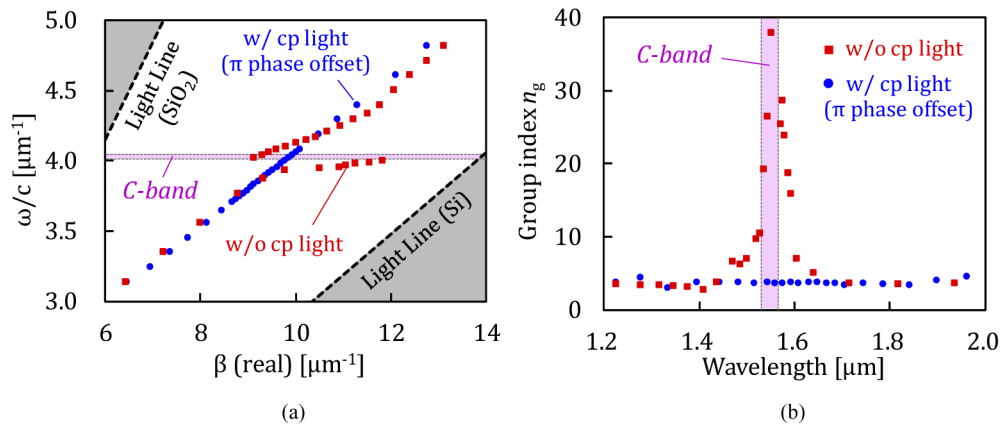


Fig. 6. (a) Calculated dispersion curves of the device without and with counter-propagating (cp) light with π phase offset, plotted along with the light lines of the SiO_2 cladding and Si core; (b) wavelength dependence of the group index n_g derived from the slope of the obtained dispersion curve.

4.2. Dispersion relation and group index of metamaterial-loaded Si waveguides without and with counter-propagating light

Using the calculated constitutive parameters of the metamaterial uniform layer, we derived the dispersion relationship and the group index of the metamaterial-loaded Si waveguide from the homogenization mode analysis with Eqs. (1)–(4). Figure 6(a) shows the dispersion relationship of the device, plotted along with the light lines of the SiO_2 cladding and the Si core (dashed black lines). The red and blue points indicate the results without and with the counter-propagating light with π phase offset, respectively. In the simulation, the Si-core width and height of the device were set to 500 and 220 nm, respectively. In addition, the distance between the Si core and the metamaterial uniform layer was set to 25 nm. When there is no counter-propagating light, the dispersion curve of the metamaterial-loaded Si waveguide shows strong nonlinearity and discontinuity in the vicinity of the resonance frequency, which reflects the sharp change in the permeability. In contrast, when the counter-propagating light with a π phase offset is incident from the opposite direction, the dispersion curve shows characteristics largely between those of the two light lines.

Figure 6(b) shows the wavelength dependence of the group index n_g derived from the slope of the obtained dispersion curve shown in Fig. 6(a). The red and blue points indicate n_g without and with the counter-propagating light with π phase offset, respectively. Without the counter-propagating light, the n_g value is greater than 60 at the resonant frequency of $1.55 \mu\text{m}$ (The device is supposed to be used for optical buffering as shown in Fig. 2, and we are considering 10-40 Gbit/s optical data transmission at $1.55 \mu\text{m}$). Under such situation, the chromatic dispersion near at $1.55 \mu\text{m}$ is within the allowable range). In addition, the delay can be significantly enhanced by increasing the number of rings, while the trade-off between the delay time and the propagation loss should be considered an important factor. With the counter-propagating light, the group index n_g is almost constant in this wavelength range and is approximately 4.2, which is consistent with that of a normal Si wire waveguide.

4.3. Slow-light control of metamaterial-loaded Si waveguides by tuning an initial phase offset of two counter-propagating incident lights

Figures 7(a) and 7(b) show the real and imaginary parts of effective permeability μ_y of the metamaterial uniform layer as a function of the initial phase offset between the two input lights,

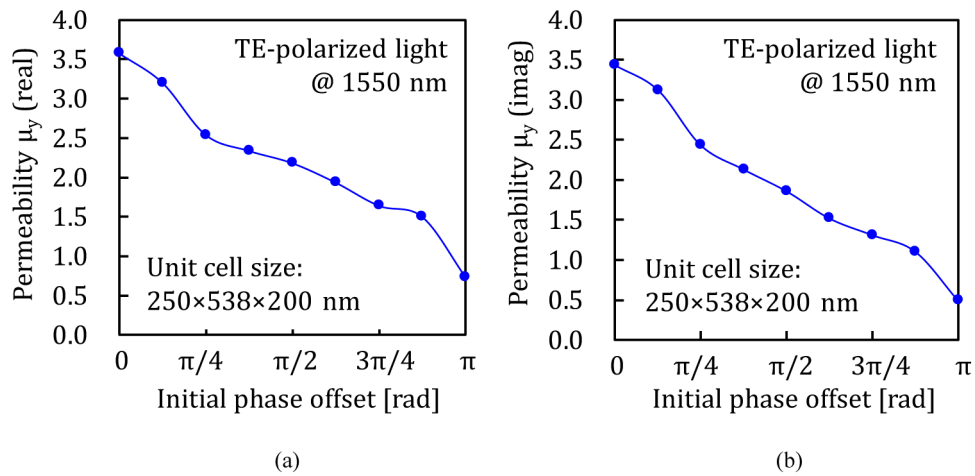


Fig. 7. Real and imaginary parts of effective permeability μ_y of the metamaterial uniform layer as a function of the initial phase offset between two input lights, calculated at a wavelength of 1.55 μm .

calculated at a wavelength of 1.55 μm . As shown in Fig. 7(a), when the initial phase offset between the signal light and the control light is 0, the real part of permeability is high (~ 3.6), because the antinode of the standing wave is located at the center of the metamaterial in the device. On the contrary, when the initial phase offset is π , the μ_y value is largely equal to that of the SiO_2 cladding layer and approaches 1, because the antinode of the standing wave is located between the metamaterials. Figure 7(a) also shows that the real part of permeability of the metamaterial uniform layer in the waveguide can be controlled continuously from 3.6 to 0.76 by changing the initial phase offset between the signal light and the control light from 0 to π . On the other hand, as shown in Fig. 7(b), the imaginary part of the permeability of the metamaterial uniform layer also changes significantly at the resonance frequency of the metamaterial, which leads to an intrinsic loss of the device loss.

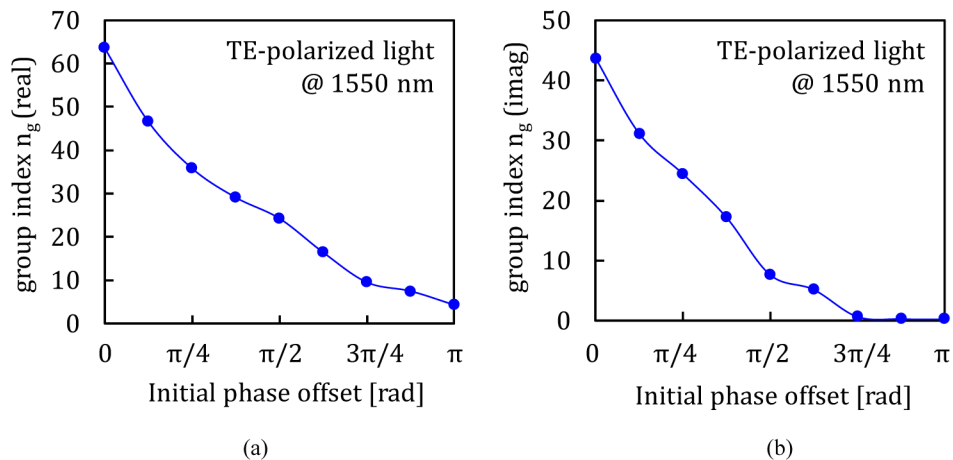


Fig. 8. Real and imaginary parts of group index n_g of the device as a function of the initial phase offset, calculated at a wavelength of 1.55 μm .

Finally, the group index n_g of the device as a function of the initial phase offset was derived from the dispersion characteristics obtained for each initial phase offset. Figure 8 shows the results. Real part of n_g can be continuously controlled from 63.6 to 4.2 at a wavelength of 1.55 μm by changing the initial phase difference between the signal light and the control light from 0 to π (Fig. 8(a)). As a result, the slow-light effect can be controlled without adding an advanced control function to the device. In addition, by changing the initial phase offset, the imaginary part of the group index (i.e. intrinsic loss of the device) also changed from 44 to 0 at a wavelength of 1.55 μm (Fig. 8(b)). When performing optical buffering using this device, it is appropriate to use the slow-light effect in a range where the imaginary part of the group refractive index is relatively small.

5. Conclusion

A metamaterial is an artificial material designed to control the electric permittivity and magnetic permeability freely beyond naturally existing values. A promising application is a “slow-light” device realized using a combination of optical waveguides and metamaterials, which can decelerate the group velocity of the guided light waves. To use the above device as a functional device, it is indispensable to dynamically control the slow-light effect with an external signal. However, once the shape of a metamaterial is decided, it is difficult to change its optical properties.

In this paper, we proposed a novel approach to control the slow-light effect. In this method, the slow-light effect (i.e., group index) is controlled by changing the phase of the control light incident on the device from a direction opposite to that of the signal light.

In this study, the dispersion relationship of the metamaterial-loaded Si waveguide was established by conducting a homogenization mode analysis to reduce the significant calculation time. Moreover, for deriving equivalent value of ϵ and μ of a unit cell including the metamaterial, we formulated from the S-parameter calculated for two counter-propagating incident light waves. From the result, by adjusting the phase offset, we confirmed that it was possible to control the amount of influence of steep chromatic dispersion by the metamaterial, the group index of the device could be continuously controlled from 63.6 to 4.2 at a wavelength of 1.55 μm .

Funding

Core Research for Evolutional Science and Technology (JPMJCR15N6, JPMJCR18T4); Japan Society for the Promotion of Science (#19H02193).

Disclosures

The authors declare no conflicts of interest.

References

1. R. A. Shelby, D. R. Smith, and S. Schultz, “Experimental verification of a negative index of refraction,” *Science* **292**(5514), 77–79 (2001).
2. J. B. Pendry, A. J. Holden, D. J. Robbins, and W. J. Stewart, “Magnetism from conductors and enhanced nonlinear phenomena,” *IEEE Trans. Microwave Theory Techn.* **47**(11), 2075–2084 (1999).
3. X. Ni, N. K. Emani, A. V. Kildishev, A. Boltasseva, and V. M. Shalaev, “Broadband light bending with plasmonic nanoantennas,” *Science* **335**(6067), 427 (2012).
4. Z. H. Jiang, S. Yun, L. Lin, J. A. Bossard, D. H. Werner, and T. S. Mayer, “Tailoring dispersion for broadband low-loss optical metamaterials using deep-subwavelength inclusions,” *Sci. Rep.* **3**(1), 1571 (2013).
5. I. M. Pryce, K. Aydin, Y. A. Kelaita, R. M. Briggs, and H. A. Atwater, “Highly strained compliant optical metamaterials with large frequency tunability,” *Nano Lett.* **10**(10), 4222–4227 (2010).
6. X. Fang, M. L. Tseng, J. Y. Ou, K. F. MacDonald, D. P. Tsai, and N. I. Zheludev, “Ultrafast all-optical switching via coherent modulation of metamaterial absorption,” *Appl. Phys. Lett.* **104**(14), 141102 (2014).
7. T. Amemiya, M. Taki, T. Kanazawa, T. Hiratani, and S. Arai, “Optical lattice model towards nonreciprocal invisibility cloaking,” *IEEE J. Quantum Electron.* **51**(3), 1–10 (2015).
8. N. I. Zheludev and Y. S. Kivshar, “From metamaterials to metadevices,” *Nat. Mater.* **11**(11), 917–924 (2012).

9. I. V. Shadrivov, A. A. Sukhorukov, and Y. S. Kivshar, "Guided modes in negative-refractive-index waveguides," *Phys. Rev. E* **67**(5), 057602 (2003).
10. N. Engheta, "Circuits with Light at Nanoscales: Optical Nanocircuits Inspired by Metamaterials," *Science* **317**(5845), 1698–1702 (2007).
11. T. Amemiya, T. Shindo, D. Takahashi, N. Nishiyama, and S. Arai, "Magnetic interactions at optical frequencies in an InP-based waveguide device with metamaterial," *IEEE J. Quantum Electron.* **47**(5), 736–744 (2011).
12. T. Amemiya, T. Shindo, D. Takahashi, S. Myoga, N. Nishiyama, and S. Arai, "Nonunity Permeability in metamaterial-based GaInAsP/InP multimode interferometers," *Opt. Lett.* **36**(12), 2327–2329 (2011).
13. T. Amemiya, T. Kanazawa, S. Yamasaki, and S. Arai, "Metamaterial Waveguide Devices for Integrated Optics," *Materials* **10**(9), 1037 (2017).
14. P. Tassin, X. Sahyoun, and I. Veretennicoff, "Miniaturization of photonic waveguides by the use of left-handed materials," *Appl. Phys. Lett.* **92**(20), 203111 (2008).
15. K. L. Tsakmakidis, A. D. Boardman, and O. Hess, "Trapped rainbow storage of light in metamaterials," *Nature* **450**(7168), 397–401 (2007).
16. H. Hu, D. Ji, X. Zeng, K. Liu, and Q. Gan, "Rainbow Trapping in Hyperbolic Metamaterial Waveguide," *Sci. Rep.* **3**(1), 1249 (2013).
17. Z. Li, M.-H. Kim, C. Wang, Z. Han, S. Shrestha, A. C. Overvig, M. Lu, A. Stein, A. M. Agarwal, M. Lončar, and N. Yu, "Controlling propagation and coupling of waveguide modes using phase-gradient metasurfaces," *Nat. Nanotechnol.* **12**(7), 675–683 (2017).
18. R. Guo, M. Decker, F. Setzpfandt, X. Gai, D.-Y. Choi, R. Kiselev, A. Chipouline, I. Staude, T. Pertsch, D. N. Neshev, and Y. S. Kivshar, "High-bit rate ultra-compact light routing with mode-selective on-chip nanoantennas," *Sci. Adv.* **3**(7), e1700007 (2017).
19. T. Amemiya, A. Ishikawa, T. Kanazawa, J. Kang, N. Nishiyama, Y. Miyamoto, T. Tanaka, and S. Arai, "Permeability-controlled optical modulator with tri-gate metamaterial: Control of permeability on InP-based photonic integration platform," *Sci. Rep.* **5**(1), 8985 (2015).
20. S. Yamasaki, T. Amemiya, Z. Gu, J. Suzuki, N. Nishiyama, and S. Arai, "Analysis of the slow-light effect in silicon wire waveguides with metamaterials," *J. Opt. Soc. Am. B* **35**(4), 797–804 (2018).
21. T. Amemiya, S. Yamasaki, M. Tanaka, H. Kagami, K. Masuda, N. Nishiyama, and S. Arai, "Demonstration of slow-light effect in a silicon-wire waveguide with a metamaterial," *Opt. Express* **27**(10), 15007–15017 (2019).
22. J. Y. Ou, E. Plum, J. Zhang, and N. I. Zheludev, "An electromechanically reconfigurable plasmonic metamaterial operating in the near-infrared," *Nat. Nanotechnol.* **8**(4), 252–255 (2013).
23. T. Driscoll, H. T. Kim, B. G. Chae, B. J. Kim, Y. W. Lee, N. M. Jokerst, S. Palit, D. R. Smith, M. Di Ventra, and D. N. Basov, "Memory Metamaterials," *Science* **325**(5947), 1518–1521 (2009).
24. K. M. Dani, Z. Ku, P. C. Upadhy, R. P. Prasankumar, A. J. Taylor, and S. R. J. Brueck, "Ultrafast nonlinear optical spectroscopy of a dual-band negative index metamaterial all-optical switching device," *Opt. Express* **19**(5), 3973 (2011).
25. S. Kocaman, M. S. Aras, P. Hsieh, J. F. McMillan, C. G. Biris, N. C. Panoiu, M. B. Yu, D. L. Kwong, A. Stein, and C. W. Wong, "Zero phase delay in negative-refractive-index photonic crystal superlattices," *Nat. Photonics* **5**(8), 499–505 (2011).
26. S. Myoga, T. Amemiya, A. Ishikawa, N. Nishiyama, T. Tanaka, and S. Arai, "Carrier-concentration-dependent resonance frequency shift in a metamaterial loaded semiconductor," *J. Opt. Soc. Am. B* **29**(8), 2110–2115 (2012).
27. H. Kagami, T. Amemiya, M. Tanaka, Y. Wang, N. Nishiyama, and S. Arai, "Metamaterial infrared refractometer for determining broadband complex refractive index," *Opt. Express* **27**(20), 28879–28890 (2019).
28. T. Amemiya, S. Myoga, T. Shindo, E. Murai, N. Nishiyama, and S. Arai, "Permeability Retrieval in InP-based Waveguide Optical Device Combined with Metamaterial," *Opt. Lett.* **37**(12), 2301–2303 (2012).
29. D. R. Smith, D. C. Vier, T. Koschny, and C. M. Soukoulis, "Electromagnetic parameter retrieval from inhomogeneous metamaterials," *Phys. Rev. E* **71**(3), 036617 (2005).